International Journal of Cardiology 203 (2016) 964–971

Contents lists available at ScienceDirect

International Journal of Cardiology

journal homepage: www.elsevier.com/locate/ijcard

# Efficient attenuation of Friedreich's ataxia (FRDA) cardiomyopathy by modulation of iron homeostasis-human induced pluripotent stem cell (hiPSC) as a drug screening platform for FRDA☆

Yee-Ki Lee [a,1], Yee-Man Lau [a,1], Kwong-Man Ng [a], Wing-Hon Lai [a], Shu-Leong Ho [c], Hung-Fat Tse [a,b,d], Chung-Wah Siu [a], Philip Wing-Lok Ho [c,*]

[a] Cardiology Division, Department of Medicine, The University of Hong Kong, Hong Kong, China
[b] Research Center of Heart, Brain, Hormone and Healthy Aging, The University of Hong Kong, Hong Kong, China
[c] Neurology Division, Department of Medicine, Li Ka Shing Faculty of Medicine, The University of Hong Kong, Hong Kong, China
[d] Hong Kong - Guangdong Joint Laboratory on Stem Cell and Regenerative Medicine, The University of Hong Kong and Guangzhou Institutes of Biomedicine and Health, China

ARTICLE INFO

*Article history:*
Received 21 September 2015
Accepted 16 November 2015
Available online 17 November 2015

*Keywords:*
Friedreich's ataxia
Induced pluripotent stem cells
Cardiomyopathy
Idebenone
Deferiprone

ABSTRACT

*Background:* Friedreich's ataxia (FRDA), a recessive neurodegenerative disorder commonly associated with hypertrophic cardiomyopathy, is caused by silencing of the frataxin (FXN) gene encoding the mitochondrial protein involved in iron–sulfur cluster biosynthesis.
*Methods:* Application of our previously established FRDA human induced pluripotent stem cell (hiPSC) derived cardiomyocytes model as a platform to assess the efficacy of treatment with either the antioxidant coenzyme Q10 analog, idebenone (IDE) or the iron chelator, deferiprone (DFP), which are both under clinical trial.
*Results:* DFP was able to more significantly suppress synthesis of reactive oxygen species (ROS) than IDE at the dosages of 25 μM and 10 nM respectively which agreed with the reduced rate of intracellular accumulation of iron by DFP treatment from 25 to 50 μM. With regard to cardiac electrical-contraction (EC) coupling function, decay velocity of calcium handling kinetics in FRDA-hiPSC-cardiomyocytes was significantly improved by DFP treatment but not by IDE. Further mechanistic studies revealed that DFP also modulated iron induced mitochondrial stress as reflected by mitochondria network disorganization and decline level of respiratory chain protein, succinate dehydrogenase (CxII) and cytochrome c oxidase (COXIV). In addition, iron-response protein (IRP-1) regulatory loop was overridden by DFP as reflected by resumed level of ferritin (FTH) back to basal level and the attenuated transferrin receptor (TSFR) mRNA level suppression thereby reducing further iron uptake.
*Conclusions:* DFP modulated iron homeostasis in FRDA-hiPSC-cardiomyocytes and effectively relieved stress-stimulation related to cardiomyopathy. The resuming of redox condition led to the significantly improved cardiac prime events, cardiac electrical-coupling during contraction.


## 1. Introduction

Friedreich's ataxia is the most common hereditary ataxia encountered in clinical practice. While the disease is well known for its neurological involvements such as progressive gait and limb ataxia [1,2], most affected individuals died prematurely due to Friedreich's ataxia related cardiomyopathy [3]. To date, no therapeutic intervention has been shown to effectively modify or alleviate the pathophysiological process. The disease is caused by GAA triplet codon expansion within the first intron of the frataxin (*FXN*) gene encoding the mitochondrial protein, frataxin, leading to heterochromatin-mediated silencing of *FXN* in affected individuals [4,5]. While controversial, it is commonly accepted that frataxin plays an important role in mitochondrial iron metabolism particularly in the biosynthesis of iron–sulfur cluster, an essential component of Complex I–III enzymes in respiratory electronic transport chain. As such therapeutic strategies have been developed primarily targeting the increased reactive oxygen species (ROS) [6–9] to possibly resume the impaired energy generation related to these pathways. For instance, idebenone (2,3-dimethoxy-5-methyl-6-(10-hydroxydecyl)-1,4-benzoquinone), a structural analog of co-enzyme Q10, shuttling electrons from Complex I and II and other flavoprotein dehydrogenase to Complex III of the mitochondrial respiratory chain [10,11] as well as acting an ROS scavengers, [12] have been demonstrated protective

☆ These authors take responsibility for all aspects of the reliability and freedom from bias of the data presented and their discussed interpretation.

* Corresponding author at: L08-33B, Laboratory Block, University Department of Medicine, Li Ka Shing Faculty of Medicine Building, The University of Hong Kong, 21, Sassoon Road, Hong Kong, China.
*E-mail address:* hwl2002@hku.hk (P.W.-L. Ho).

[1] These authors contribute equally to this work.

http://dx.doi.org/10.1016/j.ijcard.2015.11.101

effects in cellular and animal models of Friedreich's ataxia. However, subsequent clinical trials have failed to demonstrate the efficacy of idebenone in Friedreich's ataxia patients with any meaningful clinical benefit of the therapy [13], thus raising the possibility whether the increased oxidative stress and the impaired ATP production are the key pathological mechanisms to the clinical phenotypes or just an epiphenomenon. In fact, this could also be related to the lack of an appropriate-yet-reliable disease model that could be recapitulating the pathophysiological process and allowing functional validation of candidate drugs. Using human induced pluripotent stem cells (hiPSCs) derived cardiomyocytes generated from patients with Friedreich's ataxia, we have previously reported that the enhanced iron uptake via upregulated transferrin receptor 1 and the resultant iron accumulation has a key pathophysiological role to induce downstream cardiomyopathic changes such as the reduced ATP synthesis, the increased reactive oxidative species (ROS) production, and the impaired calcium handling properties [14]. Based on our previous findings, we hypothesize that iron chelating could be one of the alternatives for treatment of FRDA by modulation of iron homeostasis. The orally active, iron chelating drug, deferiprone (DFP, 1, 2 dimethyl-3-hydroxy-pyrid-4-one) and its derivatives were primarily designed and screened for the treatment of iron overload and toxicity conditions [15]. They were identified as powerful free radical damage inhibitor since 30 years ago [16] and many *in vitro*, *in vivo* and clinical studies have confirmed these results [17,18]. Nevertheless, the studies of DFP and its derivatives were limited in neuroprotective effects [19].

In the present study, we exploited our previously established hiPSC-cardiomyocyte based Friedreich's ataxia model as a drug-testing platform to compare relative efficacy of the antioxidant, idebenone (IDE), Co-enzyme Q10 analog and an iron chelator, deferiprone (DFP), on mitochondrial function, reactive oxidative species production and calcium handling properties. Our results not only provide pathophysiological insights to therapeutic strategy for treatment of Friedreich's ataxia related cardiomyopathy, but also more importantly our approach illustrates that hiPSC-based drug testing strategy can be an integral part of future pre-clinical drug development.

## 2. Methods

### *2.1. Generation of human induced pluripotent stem cells and their cardiac derivatives*

Skin biopsies were obtained under standard aseptic technique from a patient with Friedreich ataxia and documented GAA triplet repeat expansions within the first intron of the *FXN* gene and one healthy age- and sex-matched control subject. Detailed methods on hiPSC generation and characterization, and in vitro cardiac differentiation have been previously reported [14,20–22].

### *2.2. Cardiac differentiation*

To induce cardiac differentiation, undifferentiated hiPSCs were maintained in mTeSR™1 medium (STEMCELL Technologies Inc., Vancouver, BC, Canada) as previously described [23–25]. Four days prior to induction, hiPSCs were dissociated into single cells with accutase (Invitrogen, CA, USA) and then seeded onto 12-well matrigel-coated plate (Thermos Scientific Inc., Walham, MA, USA) supplemented with Y27632 (5 μM) (Stemgent, Cambridge, MA, USA). On the first induction day, the culture medium was switched to RPMI medium (Life Technologies, Maryland, USA) without insulin and supplemented with B27 (Life Technologies, Maryland, USA) and a GSK-β inhibitor, CHIR99021 (12 μM) (Selleckchem, Houston, TX, USA), which was refreshed 24 h later. On Day 4, a Wnt signaling inhibitor, IWP2 (5 μM) (Selleckchem, Houston, TX, USA), was added to the culture medium. Typically, spontaneously beating cardiomyocytes could be observed around 9 days after induction. The cells were maintained in the culture and were dissociated approximately 30 days after induction using 0.25% Trypsin-EDTA for further experiments.

### *2.3. Friedreich's ataxia related cardiomyopathy model*

To recapitulate the cellular features of Friedreich ataxia cardiomyocytes, hiPSC-derived cardiomyocytes were cultured for 48 h in a medium supplemented with 200 μM iron (II) sulfate as previously described [14]. Iron content of hiPSC-derived cardiomyocytes was assayed with rate fluorescence quenching of calcein by iron. The dissociated cardiomyocytes from iPSCs were plated onto a 96-well white microtiter plate. Calcein-AM (Life Technolgies, Maryland, USA) was dissolved in DMSO with a stock concentration of 10 mM. The dissociated cardiomyocytes were incubated in 10 μM calcein-AM in 5% FBS cardiomyocytes maintenance medium for 15 min, and washed twice with fresh medium before recording by M200 plate-reader (Tecan, Männedorf, Switzerland) for every 5 min. The intracellular iron (II) ion levels were expressed as reciprocal of the initial rate of fluorescence intensity rise.

### *2.4. Drug testing*

To test the potential therapeutic effects, idebenone (Sigma-Aldrich, St. Louis, MO) and deferiprone (Selleckchem, Houston, TX, USA) were dissolved in DMSO at stock concentration 50 mM, stored at −20 °C, and were freshly diluted to the test concentration according to previous viability testing [6].

### *2.5. Reactive oxygen species (ROS) assay*

hiPSC-derived cardiomyocytes treated with iron (II) sulfate for 48 h were seeded into a 96-well black microtiter plate at a density of $2 \times 10^4$/well. The ROS contents in hiPSC-derived cardiomyocytes were determined using DCFDA Cellular ROS Detection Assay Kit (Abcam, Cambridge, UK) according to manufacturer instructions. Briefly, hiPSC-derived cardiomyocytes were washed with DPBS and incubated with 25 μM DCFDA mix for 45 min at 37 °C in dark. Cells were then washed once with buffer solution before drug treatment. The signal was then detected every 5 min by M200 plate-reader (Tecan, Männedorf, Switzerland) with excitation wavelength at 485 nm and emission at 535 nm. Columns of non-stained cells were reserved as blank control.

### *2.6. Measurement of intracellular calcium homeostasis*

Cytosolic calcium transients were measured in isolated hiPSC-derived cardiomyocytes using a confocal imaging system (Olympus Fluoview System version 4.2 FV300 TIEMPO) mounted on an upright Olympus microscope (IX71) as previously described as previously described [24,26–28]. Briefly, cells were loaded with 1:1 (v/v) amount of 20% Pluronic®-F127 (Invitrogen, life technologies) and 5 μM Fluo-3 AM (Sigma-Aldrich, St. Louis, MO) dissolved in DMSO with stock concentration of 5 mM for 45 min at 37 °C in Tyrode solution containing 140 mM NaCl, 5 mMKCl, 1 mMMgCl2, 1.8 mM CaCl2, 10 mM glucose and 10 mM HEPES at pH 7.4. Calcium transients of single cardiomyocytes were recorded with a temporal resolution of the line scan at 274 frames per second. All confocal calcium imaging experiments were performed within 48 h after isolation in order to minimize contamination of time-dependent changes in calcium handling property in culture. Fluorescence intensity was recorded by area against time mode (XYT) as a line plot, the calibration curve showed that there is linear relationship between fluo-3 intensity recorded with calcium concentration up to 630 nM [$Ca^{2+}$]. The data were then quantified as the background subtracted fluorescence intensity changes normalized to the background subtracted baseline fluorescence using Image J (National Institutes of Health. Amplitudes, maximal upstroke and decay velocity of calcium transient were analyzed by Clampfit version 9.2.0.09. (Axon Instruments, Inc., Foster City, CA).

### 2.7. MitoROS staining of mitochondria

The dissociated cardiomyocytes were seeded onto 2 mm glass coverslip and incubated for 48 h. Staining of mitochondria was revealed by adding 10 μM of mitoROS (Molecular probes) dissolved in DMSO in HBSS buffer containing 1% FBS. The cells were further stained for 15 min at 37 °C and 5% $CO_2$. Briefly, washed the cells with HBSS staining buffer and fixed the cells in 4% paraformaldehyde. The cells were then mounted onto Flurosave hydrophilic mountant (Merck Millipores, Billerica, MA, USA) after staining with DAPI.

### 2.8. Immunoblotting of mitochondrial protein and ferritin

Mitochondrial fraction was prepared by kit from abcam (Cambridge, MA). In brief, the freezed cell pellet with one million of cardiomycoytes was lysed by Doune's homogenizer for 20 strokes in 0.5 mL reagent A. The lysate was spinned with 100 g for 5 min while the supernatant was collected. The remaining pellet that was lysed again in reagent B is further subjected to spinning.

Regarding the whole cell lysis, the cells were washed with DPBS, and collected in RIPA buffer (Cell Signaling Technology, Danvers, MA) containing 0.2% Triton X-100, 5 mM EDTA, 1 mM PMSF, 10 μg/mL leupeptin, 10 μg/mL aprotinin, with additional 100 mM NaF and 2 mM $Na_3VO_4$ and lysed for 30 min on ice. The supernatant was collected after spinning for 20 min at 12,000 g. Protein assay was performed using a Bio-Rad protein assay kit (Hercules, CA).

Five microgram of resultant protein lysate was loaded into Bolt® 4–12% Bis-Tris plus gel (Gibco) and were transfer by transblot system onto nitrocellulose membranes and blocked with 5% non-fat dry milk in TBS [pH 7.4] with 0.5% Tween-20 at 4 °C. The transferred protein will be probed by primary mouse monoclonal antibodies to flavoprotein (FP) subunit of succinate dehydrogenase (SDH) (CxII or SDHA) (Cat no: ab14715; Abcam, Cambridge, UK, 1:2000) and rabbit polyclonal antibodies against (COXIV) (Cat no: ab16056; Abcam, Cambridge, UK, 1:5000) as a mitochondrial loading control and were further visualized by secondary HRP antibodies (Cell Signaling Technology, Danvers, MA; 1:2000).

### 2.9. Reverse transcription quantitative polymerase chain reaction (RT-qPCR)

Total RNA from hiPSC-cardiomyocytes was extracted with TRI regent (Life Technologies). Reverse transcription was then performed using 1 μg RNA in a final volume of 20 μL, using QuantiTect® reverse transcription kit (Qiagen, Hilden, Germany, http://www1.qiagen.com) according to the manufacturer's instructions. Quantitative PCR analysis was performed with real-time PCR system (StepOne Plus Reall Time PCR systems, Applied Biosystems) using the Fast SYBR Green Reagent (Qiagen). For amplification, after initial holds for 5 min at 95 °C, 40 cycles of 95 °C for 30 s followed by corresponding annealing temperature for 30 s and 72 °C for 30 s, melt curve analysis was performed. The relative quantification of PCR products was performed according to the $2^{-\Delta\Delta Ct}$ method, using mouse GAPDH as internal control. Where $\Delta\Delta Ct = [(Ct_{\text{target gene}} - Ct_{GAPDH})_{\text{Treatment group}} - (Ct_{\text{target gene}} - Ct_{GAPDH})_{\text{Control group}}]$.

### 2.10. Statistical analysis

All graphs were prepared using GraphPad Prism™ 5. Results were expressed as mean ± SEM. Means of two populations were compared using Student's t-test for paired observations. Two way analysis of variance (ANOVA) was performed followed by Holm–Sidak test for all pairwise multiple comparison procedures, using SPSS (version 14.0). A value of $p < 0.05$ was considered significantly different.

### 2.11. Study approval

The study protocol of procurement of human tissue for the generation of hiPSCs was approved by the local Institutional Review Board University of Hong Kong/Hospital Authority Hong Kong West Cluster (HKU/HA HKW IRB; UW08-258) and was registered at the Clinical Trial Center, the University of Hong Kong (HKCTR-725, http://www.hkclinicaltrials.com). Voluntary prior informed consents were obtained from all participants.

## 3. Results

In the current study, we aimed to compare the effect of DFP and IDE on FRDA-hiPSC-cardiomyocytes using ROS assay and cardiac functional changes in terms of calcium handling properties. Next, we further investigated the mechanism of DFP in treatment of FRDA in the scope of mitochondrial response, iron homeostasis gene regulation and labile iron accumulation.

### 3.1. ROS synthesis and intracellular iron accumulation were significantly suppressed by DFP

Since the major deleterious effect to mitochondrial energy synthesis dynamics is affected by redox imbalance, we aimed to understand the extent of improvement in ROS synthesis from FRDA-hiPSC cardiomyocytes under iron stress using 2′,7′ –dichlorofluorescin diacetate (DCFDA) Cellular ROS Detection Assay. ROS assay is a golden standard to access redox status of a cell, in present study, we first did pilot study with the test concentrations of iron chelater, deferiprone (DFP), ranged from 25 to 50 μM, while the dosages of Co-enzyme Q10, idenbenone, were tested from 0.01 to 10 nM in log10 scale [6]. In basal condition, supplementation of iron (II) sulfate at 100 μM and 200 μM would raise the amount of ROS synthesis dose-dependently in both WT-and FRDA cells, while FRDA cells showed a more prominent surge in ROS synthesis for 32% and 65% in 100 μM and 200 μM $Fe^{2+}$ in comparison with basal condition. In basal condition, both of the wild type and FRDA-hiPSC-cardiomyocytes are responsive to treatment of DFP at the minimal dose tested at 25 μM and presented with a significant suppression of ROS production (Fig. 1A). In presence of exogenous iron (II) loading at 100 to 200 μM, the WT-cell lines are slightly responsive to idebenone in both levels of iron loading stress while FRDA-hiPSC-cardiomyocytes did not show any response to every dose of idebenone (Fig. 1B). On the contrary, DFP is able to exert a higher efficacy on suppression of ROS synthesis ranged from a minimal dose of 25 μM to 50 μM in both of the WT- and FRDA-hiPSC-cardiomyocytes. In the FRDA cells, the amount of ROS production was significantly reduced by about 52%, 62% and 60% by all dosages of DFP treated in control, 100 μM and 200 μM $Fe^{2+}$ loaded group respectively (Fig. 1A) ($n = 3$, $^{*}p < 0.005$; FA: basal vs. 25 μM DFP co-treatment with 100 μM $Fe^{2+}$: 132 ± 12% to 50 ± 9%**; basal vs. 25 μM DFP co-treatment with 200 $Fe^{2+}$: 165 ± 14 to 70 ± 7%**).

Since the stress was primarily due to oxidation of iron accumulated as a result of FXN deficiency, which plays a role in the altered iron-sulfur cluster synthesis pathway, we sought to focus on the extent of intracellular iron accumulation. A fluorescence based assay using calcein-AM dye was performed to access rate of iron accumulation in terms of bleaching of signal per minute. In baseline condition, iron accumulation rate was similar between WT-and FRDA-hiPSC-cardiomyocytes (Fig. 1C). However, iron loading for 48 h significantly increased the rate of iron accumulation in FRDA-hiPSC-cardiomyocytes for 33% (from basal 0.003 ± 0.000 to Fe-loaded condition 0.004 ± 0.000 FLU/min**, $n = 6$, $^{**}p < 0.005$) and the rate of accumulation in FRDA cells is also remarkably elevated for 14.4% in comparison with WT cells (200 μM $Fe^{2+}$: WT vs FRDA: 0.003 ± 0.000 vs. 0.004 ± 0.000 FLU/min, $n = 6$, $^{**}p < 0.005$). Consistent with our ROS assay result, DFP treatment at the lowest dose (25 μM) started to significantly suppress the rate of iron accumulation

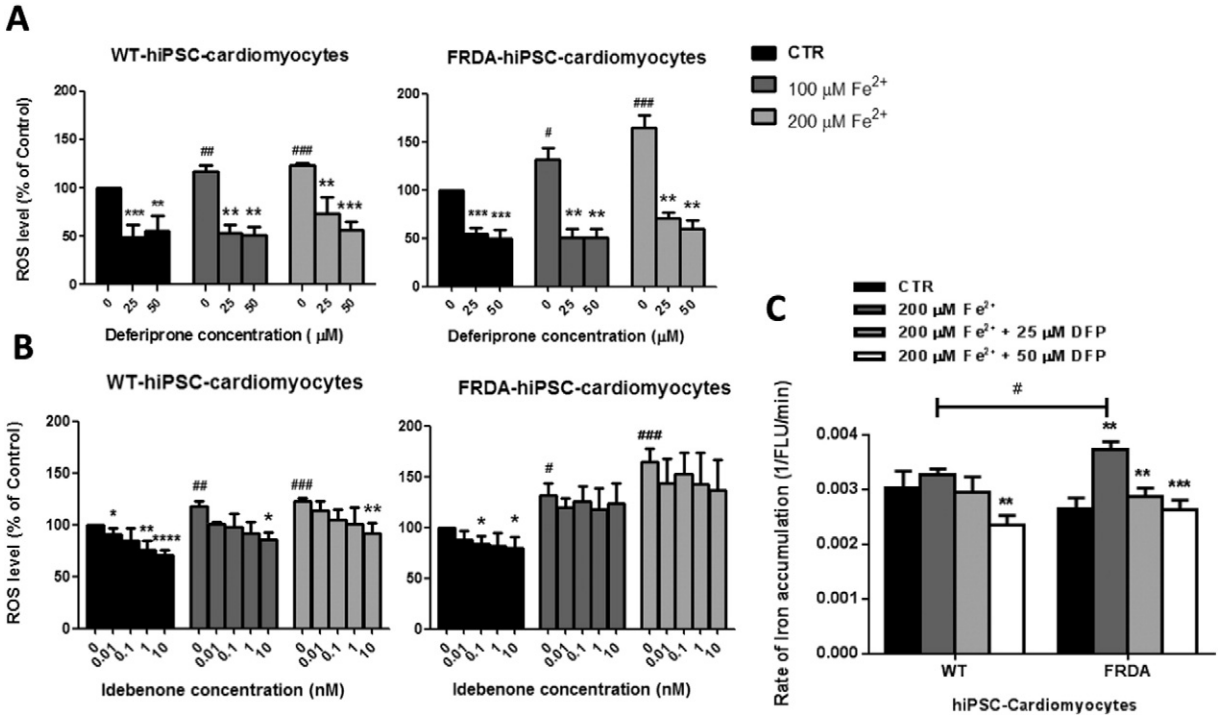


**Fig. 1.** Reactive oxygen species (ROS) assay on the effect of (A) Deferiprone (DFP) and (B) Idebenone (IDE) on $Fe^{2+}$ (200 μM) overloaded WT- and FRDA-hiPSC-cardiomyocytes. DFP is able to exert a high efficacy on suppression of ROS synthesis that ranged from a minimal dose of 25 μM to 50 μM in both of the WT- and FRDA-hiPSC-cardiomyocytes (n = 3, Control vs. 100 or 200 μM $Fe^{2+}$, $^{\#\#}p < 0.005$, $^{\#\#\#}p < 0.01$; Baseline vs. DFP or IDE treatment, $^{*}p < 0.05$, $^{**}p < 0.01$ and $^{****}p < 0.005$). (C) Rate of Iron uptake assay by calcein fluorescence bleaching in DFP-treated hiPSC-cardiomyocytes Iron overload in FRDA-iPSC cardiomyocytes. The level of intracellular iron (II) ions content is inversely proportional to the signal of the fluorescence dye, calcein-AM, since high amount of divalent iron ions will quench the fluorescence signal. The rate of intracellular iron accumulation is calculated by 1/fluorescence signal of calcein (1/FLU/min). Iron loading in FRDA-iPSC-CMC is significantly higher when it is treated with extreme amount of $Fe^{2+}$ (200 μM) (n = 6; baseline vs drug treatment: $^{**}p < 0.005$ and $^{***}p < 0.001$; WT vs. FA with $Fe^{2+}$ loading (200 μM; n = 6; $^{\#}p < 0.05$). DFP is able to significantly suppress intracellular iron (II) level.

comparable to baseline level (FA-hiPSC cardiomyocytes: from $Fe^{2+}$ to $Fe^{2+}$ + 25 μM DFP: 0.004 ± 0.000 to 0.003 ± 0.000 (n = 6; $^{**}p < 0.01$), and interestingly, the extent of reduction is in a dose-dependent manner up to 50 μM of DFP, which indicates such method is a sensitive assay to detect early event sign of stress. DFP is able to chelate the iron successfully in a remarkable manner.

### 3.2. Calcium handling of DFR treated improved calcium reuptake function

Regarding calcium handling properties of the FRDA-hiPSC-cardiomyocytes, which account for electrical-contraction function, the effect of deferiprone and idebenone was compared to evaluate the treatment efficacy to excitation-contraction (EC)-coupling process, which is highly energy demanding. The dosages of DFP at 25 μM and IDE at 10 nM and were selected for treatment of cardiomyocytes for calcium handling studies based on the dose responses to reduce ROS synthesis. Consistent with our previous studies, the upstroke and decay kinetics of FRDA-hiPSC-cardiomyocytes was significantly retarded in presence of iron stress (Fig. 2C and D). In WT-hiPSC-cardiomyocytes, IDE did not rescue calcium kinetics upon iron stress in terms of decay velocity (WT: $Fe^{2+}$ vs. $Fe^{2+}$ + IDE: −0.008 ± 0.001 vs. −0.008 ± 0.001 $F/F_o/s$) (Fig. 2D). The upstroke velocity of IDE treated cell was even retarded in presence of IDE treatment of WT cells (WT: $Fe^{2+}$ vs. $Fe^{2+}$ + IDE: 0.029 ± 0.002 vs. 0.017 ± 0.001 $F/F_o/s$). On the contrary, the decay kinetics of FA-hiPSC-cardiomyocytes with DFP treatment was significantly better than iron stressed condition despite remarkable difference was observed in wild type cell lines (FRDA: $Fe^{2+}$ vs. $Fe^{2+}$ + DFP: −0.004 ± 0.000 vs. −0.005 ± 0.000$F/F_o/s$, n = 13, $^{*}p < 0.05$) (Fig. 2D. And the unaltered level of sarcoplasmic reticulum calcium ATPase (SERCA) gene expression in the presence of iron or DFP showed that the compromised calcium decay kinetics is solely due to suppressed energy (Fig. 4C).

### 3.3. DFP relieved mitochondrial stress in terms of organization and respiratory chain protein expression in FRDA-hiPSC-cardiomyocytes

With the evidence of drug screening results from ROS synthesis and cardiac functional assay, we focused on testing of the effect of DFP in terms of mitochondrial properties which is highly vulnerable to oxidative stress. This was evaluated by studying the physical organization of mitochondrial network in the WT- or FRDA-hiPSC-cardiomyocytes visualized by mitoROS staining. In basal condition, both of the cell lines showed a well-organized network of mitochondria (Fig. 3A). Nevertheless, a sign of stress was observed in FRDA-hiPSC-cardiomyocytes when they were undergone Fe (II) stress. A prominent disorganized and fragmented mitochondrial network as well as depleted amount of mitochondria were observed (arrows; Fig. 3A).

To specifically evaluate iron-sulfur cluster containing respiratory protein level, mitochrondrial protein was extracted by *Dounce's* homogenization followed by imunoblotting (Fig. 3B). Succinate dehydrogenase (CxII) was investigated because our previous study reported that succinate-dependent ATP synthesis is vulnerable to iron loading in FRDA-hiPSC-cardiomyocytes while cytochrome c oxidase or complex IV (COXIV) is served as a marker to evaluate intact mitochondria [14]. Prominent reduction of respiratory chain protein levels in CxII isolated from mitochondrial fraction revealed the iron load condition destroyed mitochondrial content in both WT- and FRDA-hiPSC cardiomyocytes. Corresponding reduction in COXIV level presented in whole cell lysate implied a reduced amount of mitochondria upon stress condition. Interestingly, the level of CXII was dose-dependently resumed by DFP ranged

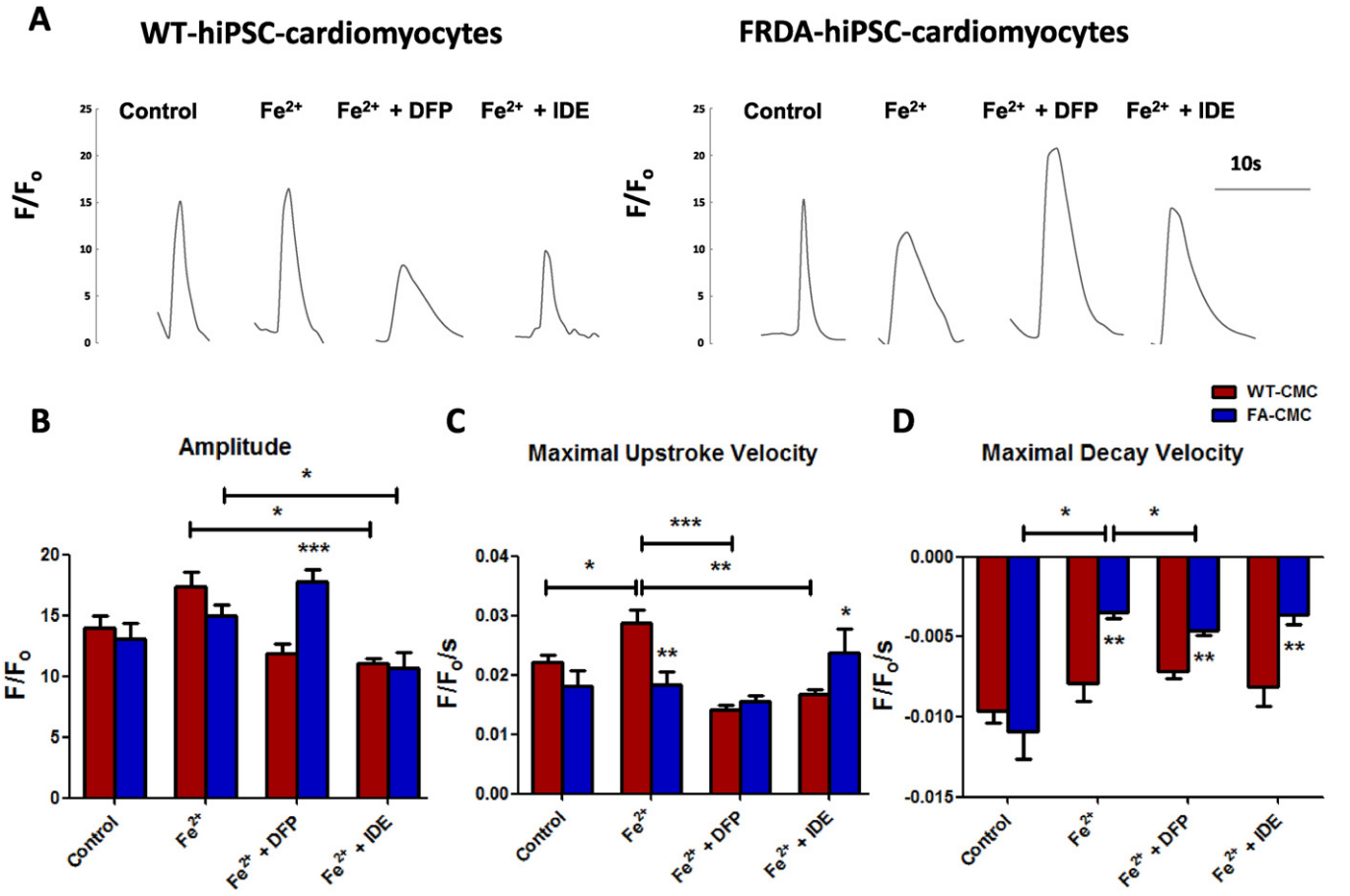


**Fig. 2.** Functional properties in the iron-loaded FRDA-iPSC-cardiomyocytes. (A) Representative tracing of calcium transients in WT-and FRDA-iPSC-cardiomycytes with DFP (25 μM) or IDE (10 nM) in presence of iron (II) loading; (B) The maximum calcium released (amplitude), (C) Vmax upstroke and (D) decay velocity ($F/F_o$/ms) (*$p < 0.05$, **$p < .005$ and ***$p < 0.0001$; WT vs. FRDA in every group of treatment or otherwise indicated by arrows) from 20 to 40 samples were presented. The iron-overloaded FRDA-iPSC-CMC presented a suppressed rate of calcium release and uptake.

from 25 to 50 μM, which indicated a resume of respiratory chain reaction. In both WT and FA cells, cytosolic levels of ferritin (FTH1), a detoxification protein as an indicator of intracellular iron level, were surge in the presence of iron loading. Both dosages of DFP reduced level of ferritin in spite of iron overload condition, the detoxification action exerted by FTH1 may no longer be necessary.

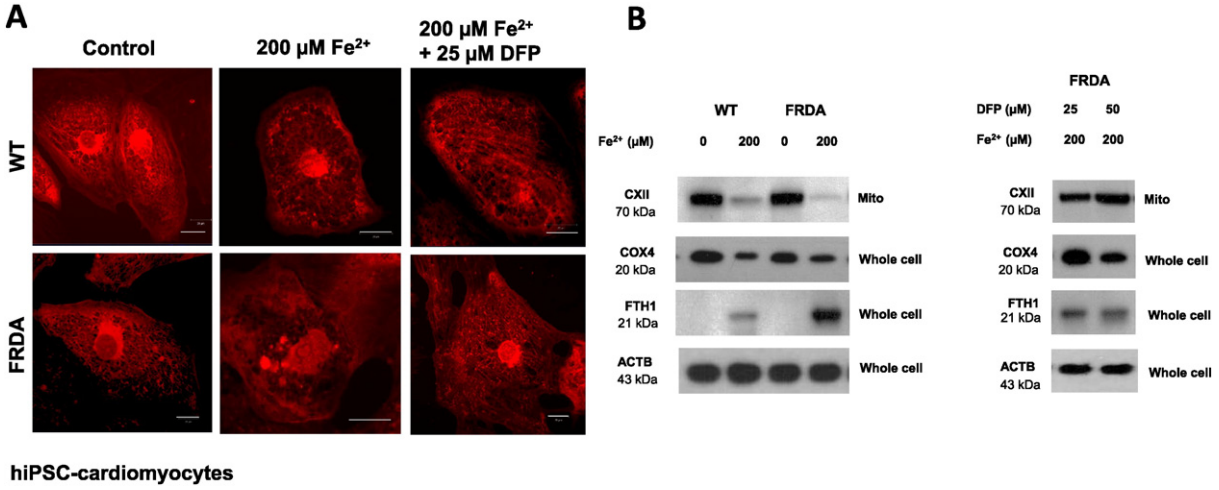


**Fig. 3.** Mitochondrial responses to DFP treatment of FRDA-hiPSC-CMC. (A) Sign of stress was indicated by fragmented organization of mitochondria network of FRDA-hiPSC-CMC overloaded with iron. (B) Immunoblot showing $Fe^{2+}$ overload induced down regulation of respiratory chain protein, succinate dehydrogenase (SDHA) CXII and mitochondrial membrane protein, cytochrome c oxidase (COX IV) in mitochondrial fraction (mito) and whole cell lysate could be resumed by DFP treatment dose-dependently in FRDA-hiPSC-cardiomyocytes. Whole cell level of Ferritin (FTH1) was declined with treatment of DFP under iron-overload condition. The cells were stressed by preloaded with $Fe^{2+}$ (200 μM) for 48 h before treatment with DFP for 24 h the dosages ranged from 25 to 50 μM. The protein lysate was prepared by mitochondrial fractionation or from whole cell with 5 μg loaded into each lane of the 4–20% gel. The COX4 would be served as a normalization control of mitochondria abundance in the cell since FRDA only affect Complex I, II and III synthesis in the respiratory transport chain.

### 3.4. Gene regulation of frataxin (FXN), transferrin receptor (TSFR), sarcoplasmic reticulum calcium ATPase (SERCA) and iron homeostasis protein, and mitochondrial carrier protein ¾ (MRSC3/4)

Frataxin gene expression significantly silenced in FRDA-hiPSC-cardiomyocytes was independent to $Fe^{2+}$ stimulation (Fig. 4A). When it comes to iron homeostasis, transferrin receptor (TSFR), the transferrin-bound iron transporter, was suppressed in response to iron loading and FRDA-hiPSC-cardiomyocytes were less responsive to the regulated suppressed TSFR gene expression level which is consistent with our previous findings (Fig. 4B). Interestingly, DFP is able to slightly relieve the level of suppression possibly due to maintenance of lower intracellular $Fe^{2+}$ loading by the chelator. Surprisingly, in both cell lines, the mitochondrial carrier proteins (MRS3/4), which govern mitochondrial uptake of $Fe^{2+}$ from cytosol to mitochondrial region for synthesis of Fe–S cluster, were elevated in the presence of iron load (WT: CTR vs. $Fe^{2+}$: 0.863 ± 0.06 vs. 1.132 ± 0.197*; FA: CTR vs. $Fe^{2+}$: 0.813 ± 0.070 vs. 1.188 ± 0.197-fold of gene expression of WT-hiPSC-CMC; $n = 5$, $^*p < 0.05$) (Fig. 4D) meaning that the iron was kept loading into mitochondrial compartment though there is reduced amount of trasferrin bound iron uptake from extracellular region into cytosol. Mitochondrial iron loading may not be relevant to extracellular iron abundance, but is possibly related to intracellular iron accumulated levels as indicated in the above data shown in calcein fluorescence bleaching assay (Fig. 1C). FRDA cells tended to accumulate more intracellular iron but the mitochondrial iron amount remains unknown in the current study. We could not observe obvious change with mitochondrial iron transporter gene expression between WT-and FRDA cells upon iron loading.

## 4. Discussion

To address the iron misdistribution with enhanced iron concentrations in mitochondria and relative cytosolic labile iron depletion, the use of membrane-permeable iron chelators, for example, deferiprone, has been considered [29,30]. This drug has been widely used for oral prescription of the treatment of beta-thalassemia [31–35]. Deferiprone was tested in a pilot, open-label study and in a randomized, placebo-controlled phase II clinical trial. Although in the pilot study deferiprone reduced an MRI signal indicating iron overload, the phase II study failed to demonstrate an improvement of ataxia, which was even worsened by high doses of the drug. However, deferiprone was able to reduce heart hypertrophy at all tested doses [30,35].

Iron-overload cardiomyopathy mediated by Fredriech's ataxia is one of the major causes of heart failure as a consequence of diastolic dysfunction, increased arrhythmic risk and late stage dilated cardiomyopathy [5]. Such iron-induced oxidative damage in disease condition has been linked to increased cardiomyocytes loss due to apoptosis and altered cellular metabolism. The iron-mediated stimulation of cardiac fibrosis would also lead to abnormal impulses conduction. Current therapeutic approaches to treat FRDA have become utmost crucial which mainly include: 1) Strategies to increase frataxin mRNA expression by decreasing heterochromatin formation at the GAA repeat to counteract gene silencing [5,36–38]; 2) methods to chelate iron and thereby reduce associated oxidative stress [39,40]; 3) to use antioxidative reagent that reduces ROS stress (36).

By taking advantages of our experience in utilization of FRDA-iPSC-cardiomyocytes model that recapitulated cardiomyopathy phenotypes in iron overload condition [14], in our current study, we successfully established a drug screening platform to identify potential candidates that ensure proper functioning of mitochondria so as to maintain normal heart function. Gene manipulation strategy was not preferable for clinical application because of the labor intensive protocol and potential safety issue concerning off target activities or viral gene transfer. Therefore, the iron chelator, derferiprone (DFP), was chosen as one of the potential agents for FRDA treatment because the disease mechanism was proposed as dependent on iron homeostasis as previously described [14]. Lastly, we also tested the effect of Co enzyme Q10, idenbenone (IDE), as a antioxidative strategies to relieve ROS burden of FRDA cells.

In the present study, iron induced ROS synthesis was more significantly suppressed by DFP than IDE in FRDA-hiPSC-cardiomyocytes.

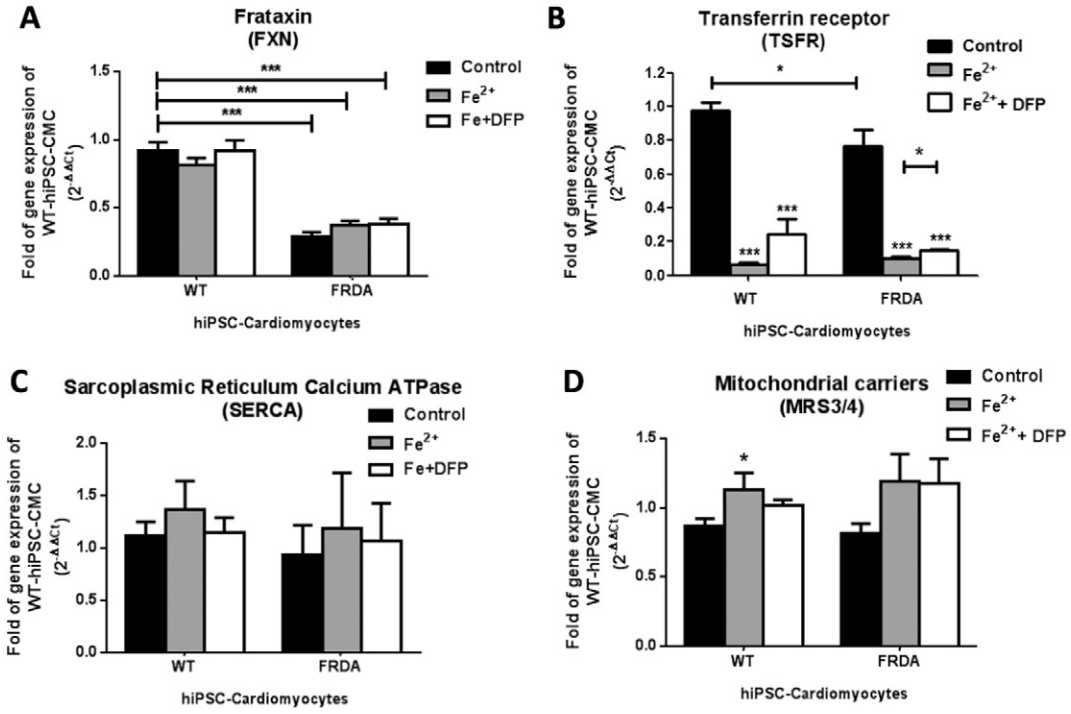


**Fig. 4.** (A) Iron loading does not alter gene expression of frataxin (FXN) and (C) calcium handling protein, SERCA (B) but leads to suppression of crucial iron homeostasis protein, transferrin receptor (TSFR) and (D) elevation of the mitochondrial carrier protein (MRS3/4). DFP treatment significantly elevated the depleted TSFR gene expression level in FRDA and showed a similar tendency in WT group as well (FRDA: $Fe^{2+}$ vs. $Fe^{2+}$ + DFP, $^*p < 0.05$, $n = 3$). qPCR determination of gene level was calculated by ΔΔCt method with treatment group comparing with baseline of each cell line or otherwise indicated with arrows, was significantly reduced upon iron (II) stress in both WT- and FRDA-iPSC-CMCs ($n = 3$, $^*p < 0.05$ or $^{***}p < 0.005$).

Iron chelation would be more significant to maintain redox balance of the cell (Fig. 1). Further investigation of FRDA therapy was focus on the lowest dosage of DFP to relieve ROS level at 25 μM to dissect the detailed mechanism. Since electrical coupling (EC) coupling process is highly sensitive to redox changes, the beneficial effects of DFP were extrapolated to cardiac function in terms of calcium handling properties with the upstroke and decay velocity of FRDA cell improved by DFP (Fig. 2C and D). This implied that SERCA function retarded by iron overload could be more efficiently resumed by DFP [37].

Indeed, excessive dosages of idebenone were proved to be harmful to skin fibroblasts of FRDA patients [40–42]. On the contrary, DFP is able to enhance redistribution of iron to a normal status. IDE only exerted a weak effect because it is not involved in iron regulation. Upon severe iron stress or in clinical situation, if the aged patient with iron accumulated exceeding threshold level, typical cardiomyopathy or neuron dysfunction would be developed, making the Co-Q10 drug may no longer work.

With respect to iron homeostasis and mitochondrial responses, in FRDA condition, loss of frataxin results in the induction of iron accumulation as indicated by our calcein bleaching assay which showed exogenous iron loading (200 μM) was able to significantly induce its accumulation (Fig. 1C). These results possibly agreed with Pandolfo's claims that inefficient Fe–S cluster biogenesis in FRDA leads to homeostasis response resembling iron deficiency, since the cells sense there is not enough building blocks for respiratory chain protein synthesis [30]. In fact apart from that, high ROS level impedes Fe–S cluster synthesis would worsen iron accumulation condition [43]. As a consequence, unbalanced intracellular distribution of the irons occurs, and iron entering into cytosol may be directly shuttled into mitochondria, where it accumulates. Furthermore, slight supplementation of iron may be beneficial to treatment because iron deficiency would worsen the disease progression due to more aggressive uptake of iron by a false signal sense in disease condition [36,44]. Our results were also agreed with clinical studies with the cohort of thalassemia patients treated with oral DFP undergoing less myocardial iron burden and better global systolic ventricular function comparing with the patients treated with the other two types of iron chelator oral deferasirox or subcutaneous desferrioxamine [31,32,35]. This could be explained by the fact that the iron chelator, DFP, is able to enter mitochondria and redirect iron to other cell compartment. However, with other kinds of iron chelator that do not favor membrane permeation, only cytosolic iron was depleted that may further boost iron uptake with into mitochondria.

As a consequence of excessive iron uptake in FRDA cell, the excessive ROS synthesis destroyed mitochrondrial function with disorganized mitochondrial network by mitoROS staining (Fig. 3A) and depletion of respiratory chain enzyme CxII and COXIV on the inner membrane (Fig. 3B) as revealed by the protein immunoblot of mitochondrial fraction and whole cell lysate respectively (Fig. 3A and B). The altered level of COXIV, an internal control of mitochondria, might probably be related to depletion of mitochondria number within the cardiomyocytes. The sign of iron overload stress was significantly relieved by DFP in a dose dependent manner in the aspect of protein level of respiratory enzyme and the reduced surge in ferritin (FTH1), the iron detoxification protein in cytosol. Such condition might be due to impeded oxidation of ferrous Iron ($Fe^{2+}$) derived from labile iron pool oxidation which generate considerable amount of hydroxyl radicals [45].

In fact, iron homeostasis is well controlled in a strictly regulated manner at transcriptional level. A key iron regulator, iron responsive element binding protein 1 (IRP1), which is localized in cytosol, is also an iron–sulfur protein. IRP1 and IRP2 predominately regulate iron metabolism by binding to the iron responsive element (IRE) sequence motif, which exist in mRNA of proteins involved in iron metabolism [39]. Under physiological conditions, iron transport tightly regulated via negative feedback mechanism involving transferrin and its receptor and other iron transportors, with gene expression control downstream of IRE [5,14]. When intracellular iron level is high, IRP1 incorporates with iron sulfur clusters to interfere the binding of IRP to iron responsive elements, thus preventing further increase in intracellular iron [46,47]. However, in case of frataxin defeats, insufficient Fe–S cluster synthesis not only lead to attenuated homeostasis response such as IRP1 activation suppression of transferrin receptor, TSFR (Fig. 4B), but also increased iron uptake to mitochondrial through MRCS3/4 (Fig. 4D). However, as presented in our gene expression studies, when intracellular iron level was restored by DFP with no alternation of FXN level, the TSFR was significantly elevated as a feedback response. Nevertheless, supplementation of mitochondrial targeting iron chelator, DFP, did not alter iron stress response of MRS3/4, a putative solute transporter of the inner mitochondrial membrane. Low dose supplementation of iron to cytosolic region keeps balance and maximizes residual expression of frataxin.

## 5. Conclusion

We have identified that DFP, the mitochondrial permeable iron chelator, is a more effective drug to treat FRDA-mediated cardiomyopathy by reducing ROS burden and improving calcium handling kinetics in comparison with IDE. The decreased iron accumulation rate accounts for the reduced redox burden due to oxidation of iron (II) with corresponding mitochondrial responses. In FRDA condition, lower abundance of mitochondrial protein was found in CMC under iron stress and DFP is able to resume the respiratory chain protein, CxII and the mitochondria level in terms of COXIV. Reduced iron accumulation by DFP alleviated the suppressed TSFR gene expression. This indicated the iron homeostasis regulated by IRP-1 is altered by the attenuated negative feedback mechanism of iron uptake.

## Author disclosure statement

The authors have nothing to disclose.

## Conflict of interest

The authors report no relationships that could be construed as a conflict of interest.

## Acknowledgments

This work was supported by grants from the Hong Kong Research Grant Council (HKU 776912 M to Drs. Siu and Lau) and Hong Kong Theme-Based Research Theme (T12-705/11 to Prof. Tse and Dr. Siu).

## References

[1] G. Geoffroy, A. Barbeau, G. Breton, B. Lemieux, M. Aube, C. Leger, et al., Clinical description and roentgenologic evaluation of patients with Friedreich's ataxia, Can. J. Neurol. Sci. 3 (1976) 279–286.
[2] J.B. Schulz, S. Boesch, K. Burk, A. Durr, P. Giunti, C. Mariotti, et al., Diagnosis and treatment of Friedreich ataxia: a European perspective, Nat. Rev. 5 (2009) 222–234.
[3] R.M. Payne, The heart in Friedreich's ataxia: basic findings and clinical implications, Prog. Pediatr. Cardiol. 31 (2011) 103–109.
[4] V. Campuzano, L. Montermini, M.D. Molto, L. Pianese, M. Cossee, F. Cavalcanti, et al., Friedreich's ataxia: autosomal recessive disease caused by an intronic GAA triplet repeat expansion, Science 271 (1996) 1423–1427.
[5] D. Herman, K. Jenssen, R. Burnett, E. Soragni, S.L. Perlman, J.M. Gottesfeld, Histone deacetylase inhibitors reverse gene silencing in Friedreich's ataxia, Nat. Chem. Biol. 2 (2006) 551–558.
[6] M.L. Jauslin, T. Meier, R.A. Smith, M.P. Murphy, Mitochondria-targeted antioxidants protect Friedreich ataxia fibroblasts from endogenous oxidative stress more effectively than untargeted antioxidants, FASEB J. 17 (2003) 1972–1974.
[7] A. Rotig, D. Sidi, A. Munnich, P. Rustin, Molecular insights into Friedreich's ataxia and antioxidant-based therapies, Trends Mol. Med. 8 (2002) 221–224.
[8] J.M. Cooper, L.V. Korlipara, P.E. Hart, J.L. Bradley, A.H. Schapira, Coenzyme Q10 and vitamin E deficiency in Friedreich's ataxia: predictor of efficacy of vitamin E and coenzyme Q10 therapy, Eur. J. Neurol.: the official journal of the European Federation of Neurological Societies 15 (2008) 1371–1379.
[9] J.M. Cooper, A.H. Schapira, Friedreich's ataxia: coenzyme Q10 and vitamin E therapy, Mitochondrion 7 (2007) S127–S135 (Suppl.).

[10] M. Bentinger, M. Tekle, G. Dallner, Coenzyme Q–biosynthesis and functions, Biochem. Biophys. Res. Commun. 396 (2010) 74–79.
[11] V. Geromel, N. Darin, D. Chretien, P. Benit, P. DeLonlay, A. Rotig, et al., Coenzyme Q(10) and idebenone in the therapy of respiratory chain diseases: rationale and comparative benefits, Mol. Genet. Metab. 77 (2002) 21–30.
[12] M.S. King, M.S. Sharpley, J. Hirst, Reduction of hydrophilic ubiquinones by the flavin in mitochondrial NADH:ubiquinone oxidoreductase (Complex I) and production of reactive oxygen species, Biochemistry 48 (2009) 2053–2062.
[13] M.H. Parkinson, J.B. Schulz, P. Giunti, Co-enzyme Q10 and idebenone use in Friedreich's ataxia, J. Neurochem. 126 (Suppl. 1) (2013) 125–141.
[14] Y.K. Lee, P.W. Ho, R. Schick, Y.M. Lau, W.H. Lai, T. Zhou, et al., Modeling of Friedreich ataxia-related iron overloading cardiomyopathy using patient-specific-induced pluripotent stem cells, Pflugers Arch. (2013).
[15] G.J. Kontoghiorghes, J. Barr, P. Nortey, L. Sheppard, Selection of a new generation of orally active alpha-ketohydroxypyridine iron chelators intended for use in the treatment of iron overload, Am. J. Hematol. 42 (1993) 340–349.
[16] G.J. Kontoghiorghes, M.J. Jackson, J. Lunec, In vitro screening of iron chelators using models of free radical damage, Free Radic. Res. Commun. 2 (1986) 115–124.
[17] G.J. Kontoghiorghes, Prospects for introducing deferiprone as potent pharmaceutical antioxidant, Front. Biosci. (Elite Ed.) 1 (2009) 161–178.
[18] G.J. Kontoghiorghes, A. Efstathiou, M. Kleanthous, Y. Michaelides, A. Kolnagou, Risk/benefit assessment, advantages over other drugs and targeting methods in the use of deferiprone as a pharmaceutical antioxidant in iron loading and non iron loading conditions, Hemoglobin 33 (2009) 386–397.
[19] G.J. Kontoghiorghes, K. Neocleous, A. Kolnagou, Benefits and risks of deferiprone in iron overload in Thalassaemia and other conditions: comparison of epidemiological and therapeutic aspects with deferoxamine, Drug Saf. 26 (2003) 553–584.
[20] W.H. Lai, J.C. Ho, Y.K. Lee, K.M. Ng, K.W. Au, Y.C. Chan, et al., ROCK inhibition facilitates the generation of human-induced pluripotent stem cells in a defined, feeder-, and serum-free system, Cell. Reprogram. 12 (2010) 641–653.
[21] J.C. Ho, T. Zhou, W.H. Lai, Y. Huang, Y.C. Chan, X. Li, et al., Generation of induced pluripotent stem cell lines from 3 distinct laminopathies bearing heterogeneous mutations in lamin A/C, Aging (Albany NY) 3 (2011) 380–390.
[22] C.W. Siu, Y.K. Lee, J.C. Ho, W.H. Lai, Y.C. Chan, K.M. Ng, et al., Modeling of lamin A/C mutation premature cardiac aging using patient-specific induced pluripotent stem cells, Aging (Albany NY) 4 (2012) 803–822.
[23] X. Lian, J. Zhang, S.M. Azarin, K. Zhu, L.B. Hazeltine, X. Bao, et al., Directed cardiomyocyte differentiation from human pluripotent stem cells by modulating Wnt/beta-catenin signaling under fully defined conditions, Nat. Protoc. 8 (2013) 162–175.
[24] Y.K. Lee, K.M. Ng, W.H. Lai, Y.C. Chan, Y.M. Lau, Q. Lian, et al., Calcium homeostasis in human induced pluripotent stem cell-derived cardiomyocytes, Stem Cell Rev. 7 (2011) 976–986.
[25] K. Ng, Y. Lee, W. Lai, Y. Chan, M. Fung, H. Tse, et al., Exogenous expression of human apoA-I enhances cardiac differentiation of pluripotent stem cells, PLoS One 6 (2011).
[26] Y.K. Lee, K.M. Ng, W.H. Lai, C. Man, D.K. Lieu, C.P. Lau, et al., Ouabain facilitates cardiac differentiation of mouse embryonic stem cells through ERK1/2 pathway, Acta Pharmacol. Sin. 32 (2011) 52–61.
[27] K.M. Ng, Y.K. Lee, Y.C. Chan, W.H. Lai, M.L. Fung, R.A. Li, et al., Exogenous expression of HIF-1 alpha promotes cardiac differentiation of embryonic stem cells, J. Mol. Cell. Cardiol. 48 (2010) 1129–1137.
[28] Y.K. Lee, K.M. Ng, Y.C. Chan, W.H. Lai, K.W. Au, C.Y. Ho, et al., Triiodothyronine promotes cardiac differentiation and maturation of embryonic stem cells via the classical genomic pathway, Mol. Endocrinol. 24 (2010) 1728–1736.
[29] S. Soriano, J.V. Llorens, L. Blanco-Sobero, L. Gutierrez, P. Calap-Quintana, M.P. Morales, et al., Deferiprone and idebenone rescue frataxin depletion phenotypes in a Drosophila model of Friedreich's ataxia, Gene 521 (2013) 274–281.
[30] M. Pandolfo, L. Hausmann, Deferiprone for the treatment of Friedreich's ataxia, J. Neurochem. 126 (Suppl. 1) (2013) 142–146.
[31] S. Totadri, D. Bansal, P. Bhatia, S.V. Attri, A. Trehan, R.K. Marwaha, The deferiprone and deferasirox combination is efficacious in iron overloaded patients with beta-thalassemia major: a prospective, single center, open-label study, Pediatr. Blood Cancer 62 (2015) 1592–1596.
[32] D. Songdej, N. Sirachainan, P. Wongwerawattanakoon, W. Sasanakul, P. Kadegasem, W. Sungkarat, et al., Combined chelation therapy with daily oral deferiprone and twice-weekly subcutaneous infusion of desferrioxamine in children with beta-thalassemia: 3-year experience, Acta Haematol. 133 (2015) 226–236.
[33] M.S. Elalfy, A.M. Adly, Y. Wali, S. Tony, A. Samir, Y.I. Elhenawy, Efficacy and safety of a novel combination of two oral chelators deferasirox/deferiprone over deferoxamine/deferiprone in severely iron overloaded young beta thalassemia major patients, Eur. J. Haematol. (2015).
[34] G. Calvaruso, A. Vitrano, R. Di Maggio, E. Lai, G. Colletta, A. Quota, et al., Deferiprone versus deferoxamine in thalassemia intermedia: results from a 5-year long-term Italian multicenter randomized clinical trial, Am. J. Hematol. 90 (2015) 634–638.
[35] A. Pepe, A. Meloni, M. Capra, P. Cianciulli, L. Prossomariti, C. Malaventura, et al., Deferasirox, deferiprone and desferrioxamine treatment in thalassemia major patients: cardiac iron and function comparison determined by quantitative magnetic resonance imaging, Haematologica 96 (2011) 41–47.
[36] K. Li, E.K. Besse, D. Ha, G. Kovtunovych, T.A. Rouault, Iron-dependent regulation of frataxin expression: implications for treatment of Friedreich ataxia, Hum. Mol. Genet. 17 (2008) 2265–2273.
[37] R. Burnett, C. Melander, J.W. Puckett, L.S. Son, R.D. Wells, P.B. Dervan, et al., DNA sequence-specific polyamides alleviate transcription inhibition associated with long GAA.TTC repeats in Friedreich's ataxia, Proc. Natl. Acad. Sci. U. S. A. 103 (2006) 11497–11502.
[38] J.M. Gottesfeld, Small molecules affecting transcription in Friedreich ataxia, Pharmacol. Ther. 116 (2007) 236–248.
[39] D.R. Richardson, Friedreich's ataxia: iron chelators that target the mitochondrion as a therapeutic strategy? Expert Opin. Investig. Drugs 12 (2003) 235–245.
[40] N. Boddaert, K.H. Le Quan Sang, A. Rotig, A. Leroy-Willig, S. Gallet, F. Brunelle, et al., Selective iron chelation in Friedreich ataxia: biologic and clinical implications, Blood 110 (2007) 401–408.
[41] V. Giorgio, V. Petronilli, A. Ghelli, V. Carelli, M. Rugolo, G. Lenaz, et al., The effects of idebenone on mitochondrial bioenergetics, Biochim. Biophys. Acta-Bioenerg. 2012 (1817) 363–369.
[42] C.K. Lim, D.S. Kalinowski, D.R. Richardson, Protection against hydrogen peroxide-mediated cytotoxicity in Friedreich's ataxia fibroblasts using novel iron chelators of the 2-pyridylcarboxaldehyde isonicotinoyl hydrazone class, Mol. Pharmacol. 74 (2008) 225–235.
[43] C.J. Murphy, G.Y. Oudit, Iron-overload cardiomyopathy: pathophysiology, diagnosis, and treatment, J. Card. Fail. 16 (2010) 888–900.
[44] U. Muhlenhoff, J.A. Stadler, N. Richhardt, A. Seubert, T. Eickhorst, R.J. Schweyen, et al., A specific role of the yeast mitochondrial carriers MRS3/4p in mitochondrial iron acquisition under iron-limiting conditions, J. Biol. Chem. 278 (2003) 40612–40620.
[45] V.A. Timoshnikov, T.V. Kobzeva, N.E. Polyakov, G.J. Kontoghiorghes, Inhibition of Fe(2+)- and Fe(3+)-induced hydroxyl radical production by the iron-chelating drug deferiprone, Free Radic. Biol. Med. 78 (2015) 118–122.
[46] M.L. Wallander, E.A. Leibold, R.S. Eisenstein, Molecular control of vertebrate iron homeostasis by iron regulatory proteins, Biochim. Biophys. Acta 2006 (1763) 668–689.
[47] M.P. Horowitz, J.T. Greenamyre, Mitochondrial iron metabolism and its role in neurodegeneration, J. Alzheimers Dis. 20 (Suppl. 2) (2010) S551–S568.